

CALIBRATION OF WORLDVIEW-2 SATELLITE IMAGERY TO REFLECTANCE DATA USING AN EMPIRICAL LINE METHOD

STABEN GW^{1,2}, PFITZNER K¹, BARTOLO R¹, LUCIEER A²

¹Environmental Research Institute of the Supervising Scientist, Australia. – (Grant.Staben@environment.gov.au)

²University of Tasmania, Australia.

Abstract - Obtaining accurate quantitative information from multispectral satellite data requires the conversion of raw digital numbers (DN) to reflectance. Sensor characteristics, illumination geometry and atmospheric conditions affect the signal received by a multispectral satellite sensor. In this paper an empirical line method is used to calibrate an eight band multispectral WorldView-2 image. Correction for illumination geometry and atmospheric attenuation in the imagery was achieved by developing a non-linear relationship between top of atmosphere (TOA) spectral radiance and surface reflectance values measured from field targets, using an (ASD Inc) FieldSpecPro spectrometer. An accuracy assessment was undertaken by comparing image reflectance values against the surface reflectance values of 17 field targets. The overall accuracy based on the RMSE for the eight bands ranged between 0.69 – 2.35% with the greatest variance in the near infrared bands. The results of this study show that empirical line methods can be used to successfully calibrate WorldView-2 satellite imagery to reflectance data.

Key Words: atmospheric correction, empirical line method, WorldView-2.

1. INTRODUCTION

The Supervising Scientist Division (SSD) is an Australian Government agency responsible for ensuring the protection of the Alligator Rivers Region (ARR) from the effects of uranium mining, and encouraging best practice in wetland conservation and management. The ARR is located in the Northern Territory, Australia (Figure 1) and covers an area of ~28,000 km², including the world heritage listed Kakadu National Park (KNP). In undertaking its role, the SSD is currently developing a remote sensing framework to assess and monitor remote areas such as the ARR at a variety of spatio-temporal scales.

To enable quantitative information to be obtained from multispectral satellite sensors such as WorldView-2 factors affecting the raw digital numbers (DN) such as sensor characteristics, illumination geometry and atmospheric effects need to be removed (Smith & Milton 1999). The effects of the atmosphere vary across the optical spectrum by either adding to, or diminishing the surface radiance values recorded by the satellite sensor (Hadjimitsis et al. 2009; Karpouzli & Malthus 2003). A number of different methods have been developed to correct for the effect of the atmosphere on satellite imagery. These include image based methods (Chavez 1996), radiative transfer models (Vicente-Serrano et al. 2008) and the empirical line method (Smith & Milton 1999).

The aim of the study is to assess the ability of the empirical line method to convert multispectral WorldView-2 imagery from top of atmosphere sensor radiance (L_{TOA}) to surface reflectance (P_s) values.

The empirical line method has been used to convert at-sensor radiance values to surface reflectance for numerous multispectral satellites (Clark & Pellikka 2005; Hadjimitsis et al. 2009; Karpouzli & Malthus 2003), and airborne hyperspectral sensors (Smith & Milton 1999). It is based on establishing a relationship between L_{TOA} values and P_s values measured from calibration targets located within the image area. The P_s values of the calibration targets are measured using field spectrometers and ideally should cover the range of albedo values found within the imagery. The L_{TOA} values are then extracted from the imagery and compared with the field measured P_s values to define prediction equations to convert image derived L_{TOA} to P_s values for each waveband (Smith & Milton 1999).

The relationship between radiance and reflectance across the whole data range (0-100%) is quadratic (Moran et al. 1990). However, correction of imagery using empirical line methods typically based on a linear relationship. This is due to the fact that the relationship between radiance and reflectance between 0-70% has been found to be essentially linear, allowing interpolation with minimal error (Clark & Pellikka 2005; Moran et al. 1990).

It must be noted that calibration of imagery using the empirical line method involves the simplification of a number of significant factors (Hadjimitsis et al. 2009). The assumptions are that both atmospheric conditions and illumination intensity are uniform across the image and that the image consists of features all with lambertian reflectance properties (Smith & Milton 1999). The degree of deviation from these assumptions is an important factor affecting the accuracy of the prediction equations developed. Karpouzli & Malthus (2003) used empirical line methods to atmospherically correct IKONOS satellite data using nine pseudo invariant targets (PIFs) and reported highly satisfactory results. They highlighted the fact that the increased spatial resolution of the IKONOS sensor enabled a large number of targets to be identified, and suggested that increasing the number of calibration targets may contribute to the reduction of error between image and field measured P_s .

Three calibration panels and seven pseudo invariant features (PIFs) were used in this current work as calibration targets to define non-linear equations for each of the eight WorldView-2 multispectral bands. A further 17 validation targets were then used to assess the reliability of the prediction equations derived for each waveband.

2. METHODS

2.1 Study Area & Data

The study area is located within KNP, approximately 250 km east of Darwin, (Figure 1) which has Ramsar listed wetland sites as well as being recognised under the World Heritage Convention. In a global context, KNP is one of the largest and most environmentally diverse national parks and is managed for

conservation, tourism, and natural and cultural features and values.

On the 11th of May 2010, two WorldView-2 multispectral images were acquired covering 620 km² of the Magela Creek catchment. As the requested study area exceeded the maximum swath width of the WorldView-2 satellite, two images were acquired during the overpass. The first image (Image 1) was captured at 11:14:28 am Australian Central Standard Time (CST) with a mean off-nadir view angle of 18.3°, and the second image (Image 2) was captured approximately 13 seconds later at 11:14:41 am CST with a mean off-nadir view angle of 16.8°. Images 1 and 2 covered an area of 183 km² and 479 km², respectively, with a 40 km² overlap between the two images. The WorldView-2 satellite consists of one panchromatic band (450-800 nm) with a spatial resolution of 0.5 m (resampled from 0.46m) and eight multispectral bands; Coastal (400-450 nm), Blue (450-510 nm), Green (510-580 nm), Yellow (585-625 nm), Red (630-690 nm), Red Edge (705-745 nm), NIR 1 (770-895 nm) and NIR 2 (860-1040 nm) with a spectral resolution of 2.0 m resampled from 1.84 m.

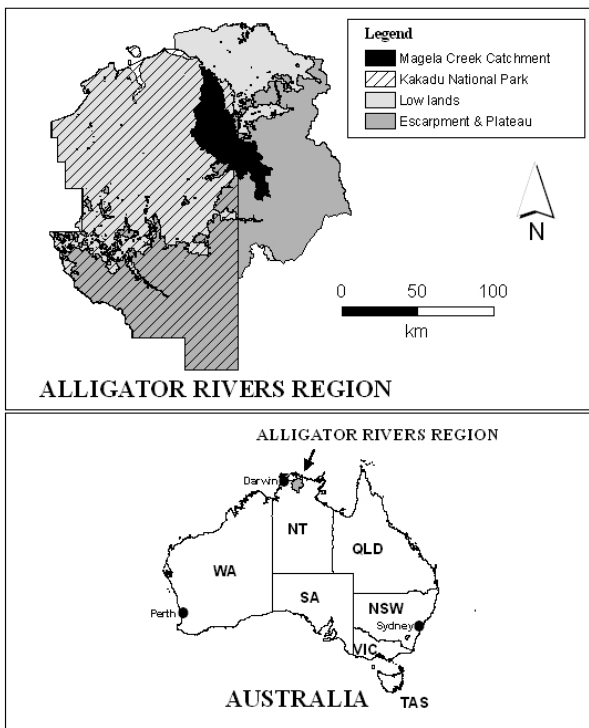


Figure 1. Location of Magela Creek Catchment.

2.2 Image pre-processing

Orthorectification of the imagery was undertaken using the sensor's Rational Polynomial Coefficients (RPC) and ground control points. A one second Shuttle Radar Topography Mission (SRTM) Digital Elevation Model (DEM) version 1 obtained from Geoscience Australia was used in the orthorectification process. Coordinates for 24 ground control points (GCPs) distributed evenly across the imagery were acquired using a dGPS (overall average positional accuracy for the X and Y coordinates was 10.6 mm). The RPC files are supplied with the imagery. Nine GCPs were used in the orthorectification of Image 2 while ten GCPs were used for Image 1. The overall accuracy assessment of the orthorectification based on six independent GCPs resulted in an

average Root Mean Square Error (RMSE) of 1.82 m. To account for sensor characteristics, the images were converted from DN to L_{TOA} spectral radiance using Eq. 1:

$$L_{\lambda Pixel, band} = \frac{K_{Band} * Q_{Pixel, Band}}{\Delta_{\lambda Band}} \quad (1)$$

Where: $L_{\lambda Pixel, band}$ represents TOA spectral radiance image pixels ($W \cdot m^{-2} \cdot sr^{-1} \cdot \mu m^{-1}$); K_{Band} is the absolute radiometric calibration factor ($W \cdot m^{-2} \cdot sr^{-1} \cdot count^{-1}$) for a given band; $Q_{Pixel, Band}$ represents the radiometrically corrected image pixels (DN); and $\Delta_{\lambda Band}$ is the effective bandwidth (μm) for a given band. The absolute calibration (K_{Band}) and effective bandwidth ($\Delta_{\lambda Band}$) parameters for each band are obtained from the metadata supplied with the imagery.

2.3 Field spectra.

This study utilised a combination of both calibration panels and PIFs to convert L_{TOA} values to P_s . Smith & Milton (1999) and Karpouzli & Malthus (2003) suggest that PIF targets used for empirical line correction should have the following characteristics: be spectrally homogenous; near lambertian and horizontal; devoid of vegetation; cover an area greater than three times the pixel size of the sensor; and cover a range of reflectance values. For this work a total of 24 PIFs were measured in the field along with three calibration panels. The three calibration panels and seven selected PIFs (Table 1) were used to derive the prediction equation between L_{TOA} and P_s for each waveband, while the remaining 17 PIFs were used as validation targets to assess the accuracy of the prediction equations (Table 2).

Table 1. Description and mean coefficient of variation for targets used in the calibration of the WorldView-2 imagery.

ID	Target description	CoV*
C1 ^c	(~1.6%) Black calibration panel	5.73
C2 ^c	(~67%) White calibration panel	2.77
C3 ^c	(~95%) Tyvec® calibration panel	0.97
C4 ^c	Sports field grass	6.96
C5 ^d	Builders Sand	6.89
C6 ^d	Sand / concrete slab	9.83
C7 ^d	Synthetic bowling green	15.58
C8 ^e	Open Water-Jabiluka billabong	9.29
C9 ^e	Open Water-Jabiluka billabong	9.31
C10 ^e	Bare earth	13.76

* Mean coefficient of variation of each target based on ASD field spectra Wavelength 400-1040 nm. Spectra collection date; (^c = 11/5/10), (^d = 13/5/10), (^e = 27/5/10).

Ideally, field reflectance spectra used to calibrate imagery should be collected at the time of image capture. However, due to numerous scheduled image capture dates proposed by DigitalGlobe combined with unseasonal adverse weather conditions, field spectra were collected on five days over a three week period during May 2010 (collection dates; 6th, 7th, 11th, 13th and 27th of May). Field spectra were collected between the hours of 10:00 and 15:00 local time using an (ASD Inc) FieldSpecPro-FR spectrometer (covering 350-2500 nm).

Spectra were captured using a 25° field of view (FoV) at nadir with the averaging sample spectrum set to 25. The sensor height was set to 1 m for targets on land and 0.5 m over water, resulting in a ground view of ~44 cm and ~22 cm in diameter, respectively. A Labsphere Spectralon® white reference panel was used to obtain reflectance data with the number of white reference readings acquired for each target dependent on the stability of the atmospheric conditions. A minimum of one and maximum of four spectral samples were collected between each white reference. The number of samples obtained for each target was dependent on the variance observed within the target, with between nine and 25 samples collected per target.

Table 2. Description and mean coefficient of variation for targets used in validation of the calibrated WorldView-2 imagery.

ID	Target description	CoV*
V1 ^a	Sports field grass	13.23
V2 ^a	Open Water Jabiru Town Lake	14.10
V3 ^a	Open Water Jabiru Town Lake	55.82
V4 ^b	Asphalt road	5.52
V5 ^b	Sports field grass	9.42
V6 ^c	Sports field grass	4.31
V7 ^c	Sports field grass	5.91
V8 ^c	Sports field grass	7.88
V9 ^c	Sports field grass	12.25
V10 ^c	Golf green	8.86
V11 ^d	Bare earth (scrape)	13.59
V12 ^d	Asphalt road	17.13
V13 ^d	Native grass	17.43
V14 ^d	Sand / Blue stone	31.86
V15 ^e	Rock outcrop	39.28
V16 ^e	Open Water Jabiluka billabong	10.18
V17 ^e	White road base	14.64

* Mean coefficient of variation of each target based on ASD field spectra Wavelength 400-1040 nm. Spectra collection date; (^a = 6/5/10), (^b = 7/5/10), (^c = 11/5/10), (^d = 13/5/10) (^e = 27/5/10).

The area sub-sampled for most targets was 25 m². However, larger areas were sampled for targets such as synthetic bowling-green, golf green, rock outcrop and bitumen road, as these targets could be easily identified within the imagery. The location of each target was recorded using a hand-held GPS with an accuracy of ±3m. The majority of targets, with the exception of the open water targets from Jabiluka billabong, were located within Image 2. The only target located within the overlap of the two images was the rock outcrop (V15 in Table 2).

The three types of calibration panels used in this project were selected as together they spanned a wide range of reflectance values. Previous laboratory spectral measurements had also shown they would be suitable targets for use as calibration panels (Pfitzner et al. 2010). The panels were laid out on the Jabiru sports field, on the morning of the satellite overpass, and spectra were collected immediately after the satellite overpass. Targets used for the prediction equation were selected based on the fact that they represented a range of reflectance values (dark to bright values), were spectrally homogenous (summarised by mean CoV) and were likely to be invariant features. The one

vegetation target used for the prediction equation was captured on the day of the image acquisition.

2.4 Empirical line calibration

The averaged field spectra (P_s) were re-sampled to the relative spectral response of each WorldView-2 waveband using the spectral re-sampling tool in ENVI 4.8 ITT Visual Information Solutions. The average L_{TOA} values associated with each calibration panel and PIF were then extracted from the imagery. A non-linear quadratic relationship Eq. (2) was fitted between L_{TOA} and P_s using the statistical software Statistica 6.1© Stat Soft, Inc:

$$y = a_1 + b_1x + b_2x^2 \quad (2)$$

where: y is the response representing P_s ; x is the predictor representing L_{TOA} ; a is the intercept; and b_1 and b_2 are the fitting coefficients. The intercept (a) represents the additive effect due to atmospheric path radiance and the slope parameters (b_1 , b_2) represent the correction for atmospheric attenuation (Hadjimitsis et al. 2009; Karpouzli & Malthus 2003).

2.5 Accuracy assessment.

The overall accuracy of the empirical line calibration was assessed by comparing image derived P_s values with field measured P_s for the 17 validation targets. Summary statistics were obtained to assess the performance of each waveband, and each individual validation target, using the RMSE Eq. (3), and the Mean Absolute Percent Error (MAPE) Eq. (4) which enables assessment of the relative error for each target. The RMSE and MAPE are computed as:

$$RMSE = \sqrt{\sum_{i=1}^n (p_i - r_i)^2} / n \quad (3)$$

$$MAPE = \frac{1}{n} \sum_{i=1}^n \left| \frac{p_i - r_i}{r_i} \right| * 100 \quad (4)$$

Where: p_i represents the predicted reflectance value; r_i represents the field measured reflectance; and n represents the number of bands (eight) for assessment of individual targets or (17) for assessment of each waveband. As the validation target V15 (rock outcrop) occurred in the overlap regions of the images, it was used to evaluate the effect that the different off nadir view angles (18.3° Image 1 and 16.8° Image 2) had on the predicted P_s values derived from each image.

3. RESULTS & DISCUSSION

3.1 Predication equations

The combination of calibration panels and PIF targets enabled the development of a non-linear relationship between L_{TOA} and P_s . A total of ten targets were used to derive the prediction equation, resulting in statistically significant relationships for each waveband ($R^2 = 0.99$, $P < 0.0001$, 99% confidence level). In common with previous studies using empirical line methods (Clark & Pellikka 2005; Karpouzli, & Malthus 2003) the correction needed for atmospheric path radiance (represented by

the intercept of the x axis) was greatest in the shorter wavelengths and decreased as wavelength increased.

3.2 Validation targets.

Summary statistics for each band are presented in Table 3. The overall RMSE values for each band show that there was a high degree of agreement between the satellite derived P_s values and field measured P_s values for the 17 validation targets. Five of the eight bands recorded RMSE values below 1.5% with the coastal band recording the lowest value (0.69%). The red-edge and two NIR bands recorded the highest RMSE values. However, the MAPE values (which assess relative error) show that red-edge band recorded similar errors to the bands in the visible portion of the electromagnetic spectrum. The increased error in the NIR bands can be attributed to the prediction equations, which produced negative reflectance values at very low L_{TOA} values.

Table 3. Summary statistics derived from the validation targets for each waveband.

Band	RMSE%	MAPE%
Coastal (1)	0.69	16.32
Blue (2)	1.00	12.87
Green (3)	1.11	8.19
Yellow (4)	1.44	13.36
Red (5)	1.48	16.31
Red Edge (6)	2.12	13.91
NIR 1 (7)	2.35	27.56
NIR 2 (8)	2.09	101.58

The WorldView-2 spectral signatures predicted for V15 (rock outcrop) from the two different off nadir view angles are presented in figure 3. The RMSE values (Image 1 = 0.57, Image 2 = 0.97) and MAPE values (Image 1 = 2.99, Image 2 = 3.33) for each image and the spectral signatures demonstrate that the prediction equations were able to account for the different view angles with very little difference in the predicted P_s values for each image.

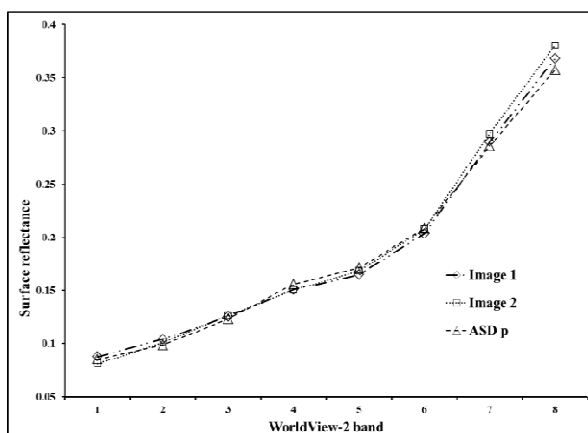


Figure 3. Comparison of the WorldView-2 spectral signature for the validation target (Rock outcrop), Image 1 and Image 2 are the predicted P_s values derived from different view angles and the ASD p is the field measured P_s .

4. CONCLUSION

The combination of both calibration panels and PIF targets enabled the development of prediction equations covering the full range of albedo values within the image. Assessment of the prediction equations based on 17 independent validation targets show that overall accuracy was high, with RMSE values between 0.69% and 2.35% across the eight multispectral bands. The results of this study show that the empirical line method using non-linear prediction equations can be used to successfully calibrate the eight multispectral bands of the WorldView-2 satellite image to surface reflectance.

REFERENCES

- P. S. Chavez, Jr. "Image Based Atmospheric Corrections – Revisited and Improved," Photogrammetric Engineering and Remote Sensing, vol. 62, p.p. 1025-1036, 1996.
- B. Clark P. Pellikka "The Development of a Land Use Change Detection Methodology for Mapping the Taita Hills, South-East Kenya: Radiometric Corrections." Proceedings of the 31st International Symposium on Remote Sensing of Environment (ISRSE), 20-24 June, St Petersburg, Russian Federation. CD-Publication, no page numbers. 2005
- D. Hadjimitis, C. Clayton, A. Retalis. "The use of selected pseudo-invariant targets for the application of atmospheric correction in multi-temporal studies using satellite remotely sensed imagery" International Journal of Applied Earth Observation and Geoinformation vol 11, p.p. 192-200, 2009.
- E. Karpouzli, T. Malthus, "The empirical line method for the atmospheric correction of IKONOS imagery," International Journal of Remote Sensing, vol. 24, p.p. 1143-1150, 2003.
- M. S. Moran, R. D. Jackson, G. F. Hart, P. N. Slater, R.J. Bartell, S.F. Biggar, D.I. Gellman, R.P. Santer, "Obtaining Surface Reflectance Factors from Atmospheric and View Angle Corrected SPOT1 HRV Data," Remote Sensing of Environment, vol 32, p.p. 203-214, 1990.
- K. Pfitzner, G. Staben, R. Bartolo, "The Spectral Reflectance of Common Artificial Pseudo Invariant Materials" Proceedings of the 15th Australasian Remote Sensing & Photogrammetry Conference (ARSPC) 13-17 September, Alice Springs, Australia. 2010
- G. M. Smith, E. J. Milton, "The use of the empirical line method to calibrate remotely sensed data," International Journal of Remote Sensing, vol. 20, 2635-2662, 1999.
- S. M. Vicente-Serrano, F. Pérez-Cabello, T. Lasanta "Assessment of radiometric correction techniques in analyzing vegetation variability and change using time series of Landsat images" Remote Sensing of Environment vol. 112, p.p. 3916–3934, 2008

Acknowledgements

We would like to thank the following: Sally-Anne Atkins, Annamarie Beradldo and John Lowry for assistance with the collection of field data, and the following people and organisations for permission to collect field data from their land/property, Traditional owners of KNP, Jabiru sports club, Jabiru Golf club, Jabiru Council and Hansons Heidelberg Cement Group.